Optical and Acoustical Methods in Science and Technology

The Fiber-Optic Sensor for the Museum Collections Protection

M. Życzkowski*

Institute of Optoelectronics, Military University of Technology, S. Kaliskiego 2, 00-908 Warsaw, Poland

The article describes the operation's rule of the fiber optic sensor in the modalmetric configuration. This type of sensor is described by comparatively simple construction, while retaining other features of fiber-optic sensors such as high sensitivity. This gives a very high potential application. In the paper possible application of the modalmetric sensor to protection of works of art and museum collections is presented. The advantage of its use is the ability to tie the fiber in structure of material. Moreover, the advantage of such type a sensor compared to existing solutions of security sensors is the reaction for vibration and touch. The paper presents the concept and results of the system optimization.

PACS: 42.81.Pa, 42.25.Bs

1. Modalmetric fiber optic sensor

A modalmetric fiber optic sensor [1], whose scheme is shown in Fig. 1, is composed of a multimode (MM) sensor fiber (1), a light source (2) for launching light into the multimode fiber to produce a multimode speckle pattern of light at an end of the fiber, a single mode fiber (3) to receive light from the multimode speckle pattern and a detector (4) connected to the single mode fiber to detect the received partial light from the multimode speckle pattern.

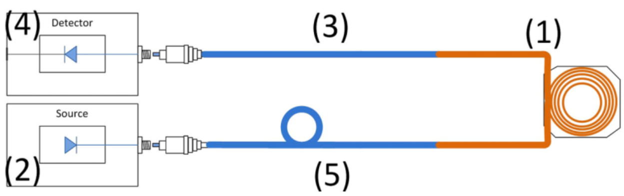

Fig. 1. Arrangement of the modalmetric sensor.

A connector connects the ends of the multimode fiber and single mode fiber with the end faces of the two fibers disposed at an acute single to one another. A modalmetric fiber sensor is based on measuring a change in the speckle pattern output of a MM fiber. When coherent light is injected into a standard MM fiber, a large number of modes are excited which will propagate down the fiber. At the output of the fiber, the interference of the modes produces a pattern known as a speckle pattern. Any disturbance to the fiber which can cause a change in any of the phase, polarization and distribution of the modes, will cause the speckle pattern to change. By measuring this change, a physical perturbation to the fiber such as a vibration or strain can be detected. The modalmetric sensor is therefore a multi-beam interferometer encapsulated within one fiber, where each beam can be represented by one of the propagating modes.

In the multimode fiber propagating modes interact with themselves along their propagation way. This interaction can be observed as stochastically stable intensity distribution at the end-face of the fiber. This distribution can be described in accordance with a Goodman proposal [2]. Goodman makes some simplifying assumptions to aid in the development of a statistical model for speckle. He assumes that the field incident at (x, y, z) is perfectly polarized and perfectly monochromatic. Under such conditions this field can be represented by a complex-valued analytic signal of the form

$$u(x,y,z;t) = A(x,y,z)\exp(\mathrm{i}2\pi\nu t), \tag{1}$$

where ν is the optical frequency and $A(x, y, z)$ is the complex phasor amplitude.

The complex amplitude of the field at (x, y, z) may be regarded as resulting from the sum of contributions from many elementary scattering areas on the rough surface. Thus the phasor amplitude of the field can be represented by

$$A(x,y,z) = \sum_{k=1}^{N} |a_k| \exp(\mathrm{i}\phi_k), \tag{2}$$

where $|a_k|$ and ϕ_k represent the amplitude and the phase of the contribution from the k-th scattering area and N is the total number of such contributions.

The directly observable quantity is the irradiance at (x, y, z), which is given by

$$I(x,y,z) = \lim_{T\to\infty} \frac{1}{T} \int_{-T/2}^{T/2} |u(x,y,z;t)|^2 \,\mathrm{d}t$$
$$= |A(x,y,z)|^2. \tag{3}$$

In a multimode fiber the light travels in several separate propagating modes, which leads to the consequence that the modes arrive to a receiver separately in time. If the optical radiation is coherent and the coherence time is shorter than the difference in the arrival time of the propagating modes, there will appear an interference pattern often called a speckle [3]. There is a need to introduce a contrast — quantity that describes discrimination of speckle intensity and can be defined as:

* e-mail: mzyczkowski@wat.edu.pl

$$V = \frac{I_{\max} - I_{\min}}{I_{\max} + I_{\min}}, \tag{4}$$

where $I_{\max}$ and $I_{\min}$ are the maximum and minimum intensity value. The speckle pattern with good contrast is more likely to reveal information than the speckle with the poor contrast. The contrast is a function of radiation source parameters (spectral radiation bandwidth Δf_{s}, mode spacing Δf_{m}, modal halfwidth δf) (Fig. 1) and the fiber parameters (mode dispersion D_{m}, fiber length L).

The transmission length of the system will depend on the relationship between laser and the optical fiber. The time delay Δt between modes determines the correlation bandwidth Δf_{c} of the multimode fiber by a formula [3, 4]:

$$\Delta f_{\mathrm{c}} = \frac{1}{\Delta t}. \tag{5}$$

Two interference patterns correlate if the bandwidth of the laser source is smaller than Δf_{c}. This indicates that if the transmission length is long enough, the time delay will be long and the correlation bandwidth will be poor, so the corresponding contrast of the overall speckle pattern is decreasing (Fig. 2) [5]. On the other hand, a laser with a narrow bandwidth results in the speckle with the high contrast.

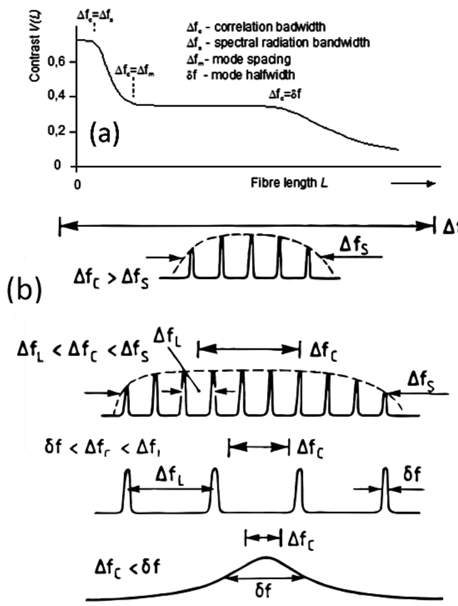

Fig. 2. The speckle pattern contrast as a function of the multimode fiber length and the source parameters (a) and its connections with the laser spectrum (b) [4].

There are many factors that influence on the contrast of the interference pattern: transmission length, correlation bandwidth, spectral radiation bandwidth, mode spacing and mode halfwidth [5]. In order to achieve high contrast for the length of the sensor, parameters of the source and the fiber optic should be properly selected taking into consideration the guidelines: number of the laser lines should be small, the laser linewidth should be narrow and the correlation bandwidth of the fiber optic should be high. Laboratory tests that summarize all aspects of the sensor configuration allowed for the optimization of sensor protection.

The detection of a perturbation using the modalmetric effect usually involves detecting a change in the speckle pattern by sampling or interrogating only part of the overall speckle pattern. This can be done through the use of physical restricting means where only part of the speckle pattern is detected, or through the use of a detector to electronically sample the required area or speckle pattern sub-zone. For this configuration, the speckle detection limit field is single-mode optic fiber (SM) which is placed before the detector. Then, any change in or redistribution of the speckle pattern will be detected as a change in intensity. Since the SM fiber supports only a single mode, it can also act as the insensitive lead-in of the sensing system.

The source radiation, converted into a multimode fiber section, undergoes further transformation on the fiber structure of the intensity distribution defined by the modal distribution described by characteristics of modal structure. Because as a receiver we consider the efficiency of single-mode fiber, which is before the detector, so input to this structure is expressed by the relation

$$\eta = \frac{2\sqrt{2}}{a w_0}\left[\frac{w}{V J_1(u)} \int_0^a J_0\left(u\frac{r}{a}\right) \exp\left(-\left(\frac{r}{w_0}\right)^2\right) r\,\mathrm{d}r + \frac{u}{V K_1(w)} \int_a^\infty K_0\left(w\frac{r}{a}\right) \exp\left(-\left(\frac{r}{w_0}\right)^2\right) r\,\mathrm{d}r\right]. \tag{6}$$

As can be seen, the efficiency of introducing of radiation to the structure of the fiber (fiber core) depends on half the diameter necking beam radiation w_0 and the fiber core radius a. This parameter allows to specify the maximum length of a transceiver single-mode fiber. Of course, the primary impact has the type, spectrum and power of radiation source.

2. Experimental setup

The scheme of the developed modalmetric sensors is shown in Fig. 3. These sensors were elaborated with the use of the different types of radiation sources (I) entering to the single-mode fiber, the sensor head in the form of several meters of multimode fiber section (II), the single-mode fiber optic cable in different lengths as a detecting fiber (III and IV).

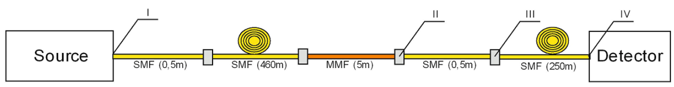

Fig. 3. The experimental setups with modalmetric sensor.

The sensor head (sensing multimode fiber optic cable) generates modal interference signal which is transmitted to the measuring and control devices through a single-mode fiber. The sensor was built using standard telecommunication optical fibers components. As the sensor output used:

a) standard telephone diode connected to an oscilloscope (type DLM 2054 — Yokogawa) to record the amplitude changes proportional to the intensity changes,

b) fiber optic spectroscopy unit (type AQ 6370C — Yokogawa) for registration of the output radiation spectrum and comparing it with the source spectrum,

c) high sensitivity HgCdTe focal plane array cameras (type SC2200-C FLIR) for laser beam profiling in any point of sensor.

To check the sensitivity of the system and to determine the frequency response of mechanical disturbance the reference system was designed and developed. This reference system was controlled with the help of a function generator (type AFG3021 Tektronix) with adjustable frequency.

3. Experimental details and results

With the use of elaborated sensor in modalmetric configuration, the response for numerous disruption of given characteristic was measured. Experimental investigation gave a series of recorded spectra. But the most important in the study was to use infrared camera. It enabled at any time for research, displaying at any point in sensor the distribution of the radiation propagating in the fiber. In this way we can test the system response to the assumed types of radiation and thereby calibrate the system for maximum response.

First, the study began with the use of telecommunication DFB laser radiation with a narrow spectrum (1550 nm wavelength). The DFB-1550-C5 series of multi quantum well (MQW) distributed feedback (DFB) lasers have been designed specifically for analog applications. Tests were carried out on the whole range of power source. In Fig. 4 measured spectral radiation, for several power levels of radiation sources, is presented.

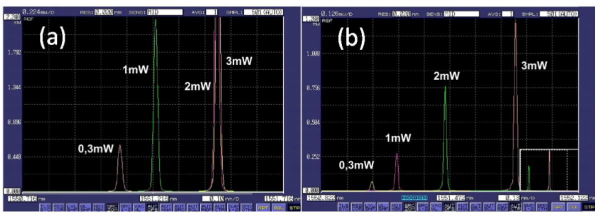

Fig. 4. The spectrum of DFB laser diode (a) and spectrum of propagating radiation in the modalmetric sensor at the multimode fiber optic cable end (b).

In the attached graphs the effect of retuning the radiation source clearly shows. In the first case (Fig. 4a) the effect is due to the expansion of the diffraction grating period with an increase in temperature caused by the increase of radiated power. In the second (Fig. 4b), the Fresnel reflections after connection the multimode fiber to the same retuning light source are observed.

During calibration, the modalmetric sensor drew attention to the spatial distribution of groups of modes propagating in a multimode optical fiber. It was to obtain a satisfactory standard result, shown in the matrix of the camera, the position of significant modes changes under the influence of vibration of the fiber. Figures 5–7 show images of optical radiation recorded at the ends of multimode fiber. There are presented the steady state and the disturbance state of sensor for different radiation power source. In each case these conditions are significantly different.

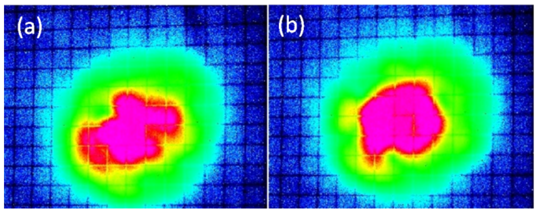

Fig. 5. Intensity distributions at the end of multimode fiber for different states of sensor: (a) steady or (b) disturbed for 0.3 mW power of source.

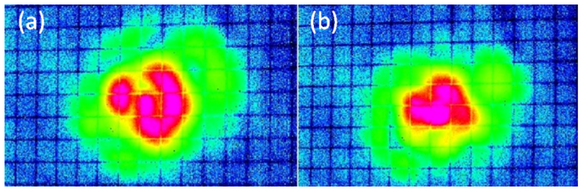

Fig. 6. Intensity distributions at the end of multimode fiber for different states of sensor: (a) steady or (b) disturbed for 2 mW power of source.

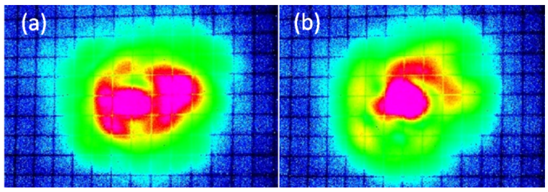

Fig. 7. Intensity distributions at the end of multimode fiber for different states of sensor: (a) steady or (b) disturbed for 3 mW power of source.

We should also add that for this type of semiconductor laser diode, for each length of tested multimode fiber, achieved the correct propagation of multimode, in which one could observe sharp group modes separation. Measuring camera software also allowed the creation of a 3D image in Matlab software as presented in Fig. 8.

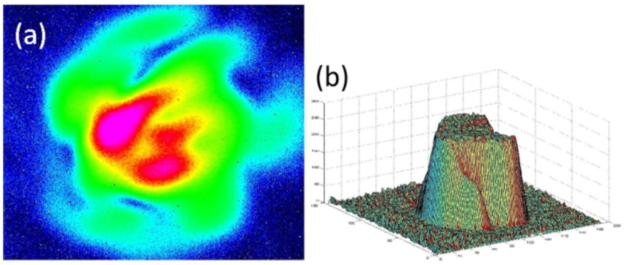

Fig. 8. Intensity distributions at the end of multimode fiber: (a) image from camera or (b) 3D-cut simulated in Matlab software.

The next research step was the registration of radiation at the end of sensor after single-mode fiber. Changes observed at the camera matrix concern intensities of light on the sensor output under the influence of forced vibrations of the fiber. The sensor was tested for single-mode fiber sections of different lengths as shown in Fig. 9 and 10. The tests results confirmed the response of the sensor to mechanical disturbances; for different lengths of optical fibers varied reaction; for a short section of SM fiber easily saturate the system (detector); recorded the strong changes, vibration, MM optical fiber. For a long section of the SM fiber system has already reacted to small disturbances. Moreover, in this configuration, the system does not saturate. This effect determines establishment of propagation conditions in the single-mode fiber. This involves a leakage of higher-order modes in the length of several meters.

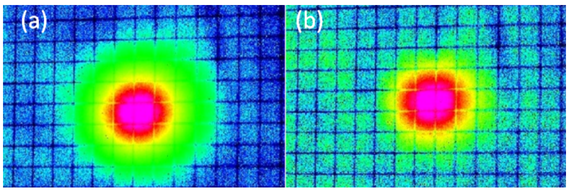

Fig. 9. Intensity distributions at the end of singlemode fiber for different states of sensor: (a) steady or (b) disturbed for 3 mW power of source and 0.5 m length of SM fiber.

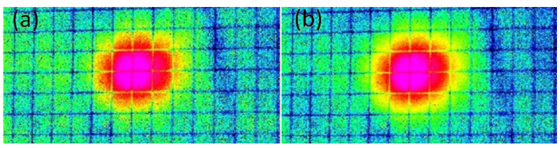

Fig. 10. Intensity distributions at the end of singlemode fiber for different states of sensor: (a) stedy or (b) disturbed for 3 mW power of source and 450 m length of SM fiber.

Finally, the tested system responds by harmonic disturbances in the structure with modulator (Fig. 4). In Figs. 11 and 12 there are presented response oscillograms of the system which was built in two sample configurations for harmonic disturbances for different frequencies.

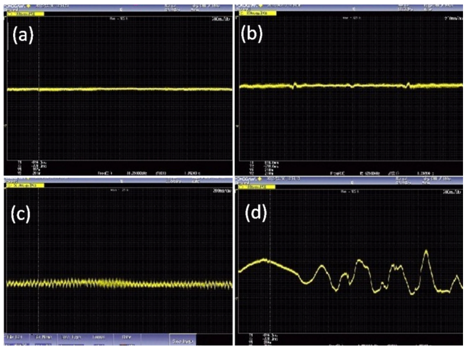

Fig. 11. Oscillograms system response to (a) steady state, (b) 1 Hz, or (c) 30 Hz, and (d) hand disorder for II configuration of modalmetric sensor (0.5 m SM fiber).

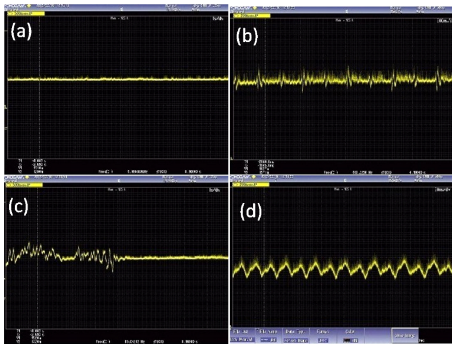

Fig. 12. Oscillograms system response to (a) steady state, (b) 1 Hz or (c) 30 Hz and (d) hand disorder for II configuration of modalmetric sensor (0.5 m SM fiber).

Another test procedure was to use a super light-emitting diode (SLED) light source. This was a 5 mW diode ESL1505-2111 type Exalos. Spectral characteristics of the diodes in each of the points of the sensor are shown in Fig. 13.

Sensor system, a SLED-powered diode was configured using the register on the camera field distribution modes. Examples of mappings of intensity distributions at the end of multimode fiber for different states of sensor are shown in Fig. 14. In contrast, shots registration system response was illustrated in Fig. 15.

The last source that was used for this study was red light diode (635 nm wavelength). In this case, the imaging modes field distribution was used with regular digital camera CCD (Fig. 16).

Finally, as in previous studies, in each configuration case, system was tested for its response to harmonic disturbances. Disturbances were generated by a mechanical modulator (Fig. 17).

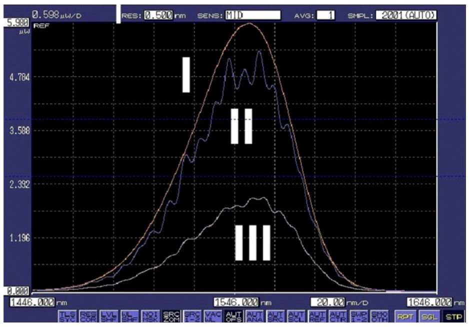

Fig. 13. The spectrum of SLED laser diode (I) and spectrum of propagating radiation in the modalmetric sensor at the MM fiber end (II) and SM fiber end (III).

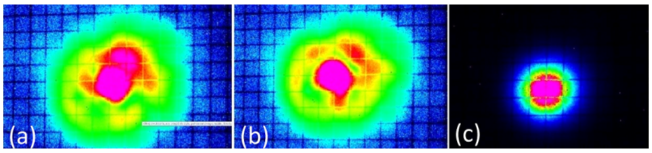

Fig. 14. Intensity distributions at the end of multimode fiber for different states of sensor: (a) steady or (b) disturbed for 5 mW power of SLED source and at the SM fiber end (c).

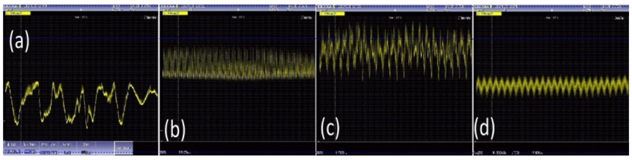

Fig. 15. Sample of oscillograms system response to (a) steady state, (b) 1 Hz, or (c) 30 Hz, and (d) hand disorder for II configuration of modalmetric sensor (0.5 m SM fiber) for the SLED-powered system.

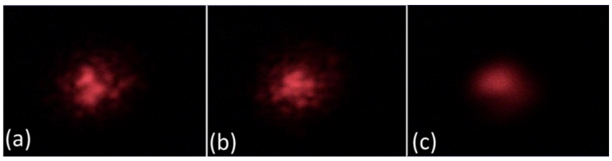

Fig. 16. Intensity distributions at the end of multimode fiber for different states of sensor: (a) steady or (b) disturbed and at the SM fiber end (c) for 5 mW power of 635 nm wavelength source.

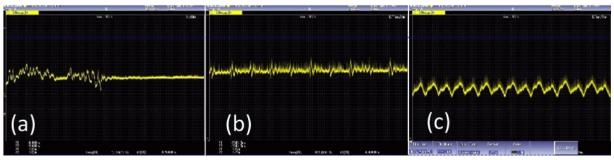

Fig. 17. Sample of oscillograms system response to (a) disturbed state, (b) 1 Hz, and (c) 30 Hz and for II configuration of modalmetric sensor (0.5 m SM fiber).

4. Conclusion

All studies and tests show that it is possible to develop a fiber optic sensor system of simple design with using the basic telecommunications elements. The sensor is sensitive to mechanical disturbances, vibrations and breaking. It will not have an ideal frequency response, but as the sensor will indicate an alarm any attempt to access the transmission medium [6–10].

In addition, because of its spatial dimensions, the use of bare fiber without coatings, it is possible to hide the sensor from accidental detection. Sensor system can be successfully integrated into the structure of the material. Therefore, we propose to use it for example to protect museum objects, where there are required: small size sensor, its discrete and effective detection of try to steal of precious relics. The study arose from need to protect one of the most valuable monuments in Poland — the coronation sword “Szczerbiec”. It is currently on display in the treasure vault of the Royal Wawel Castle in Kraków as the only preserved piece of Polish Crown Jewels.

Acknowledgments

The project co-financed by the Polish NCBiR agency. Title of project “Integrated multisensor system for monitoring and protection of sea port”. Development projects contract no. OR00002812.

References

[1] Patent number: WO 2009/111820 A1; Future Fibre Technologies PTY LTD.

[2] J.W. Goodman, *J. Opt. Soc. Am.* **73**, 66 (1976).

[3] S. Karlson, in: *29th Int. Carnahan Conf. on Security Technology, Stockholm (Sweden)*, Ed. S. Jonson, Information Gatekeepers Inc., Brighton 1994, p. 157.

[4] K. Gut, *J. Phys. IV: JP* **129**, 109 (2005).

[5] P. Schmidt, W. Stephan, *J. Opt. Commun.* **5**, 79 (1984).

[6] M. Życzkowski, M. Kondrat, W. Ciurapiński, *J. Phys. IV: JP* **129**, 189 (2005).

[7] M. Szustakowski, W.M. Ciurapinski, M. Życzkowski, *Proc. SPIE* **6736**, 131 (2007).

[8] M. Szustakowski, M. Chojnacki, M. Życzkowski, N. Pałka, *Opto-Electron. Rev.* **9**, 413 (2001).

[9] M. Życzkowski, W. Ciurapiński, M. Szustakowski, M. Kondrat, N. Pałka, *Proc. SPIE* **5566**, 300 (2004).

[10] M. Kondrat, M. Szustakowski, A. Górka, N. Pałka, M. Życzkowski, S. Niżnik, *Proc. SPIE* **5611**, 225 (2004).